

Received: 2019.05.14
Accepted: 2019.08.08
Published: 2019.12.09

The Construction of a Radiation-Induced Brain Injury Model and Preliminary Study on the Effect of Human Recombinant Endostatin in Treating Radiation-Induced Brain Injury

Authors' Contribution:
Study Design A
Data Collection B
Statistical Analysis C
Data Interpretation D
Manuscript Preparation E
Literature Search F
Funds Collection G

ABCE 1 **Chenyang Ma***
A 1 **Juying Zhou***
D 1 **Xiaoting Xu**
AC 1 **Lili Wang**
B 1 **Songbin Qin**
B 1 **Chao Hu**
F 1 **Liangqin Nie**
A 2 **Yu Tu**

1 Department of Radiotherapy, The First Affiliated Hospital of Soochow University, Suzhou, Jiangsu, P.R. China
2 School of Radiation Medicine and Protection, Medical College of Soochow University, Suzhou, Jiangsu, P.R. China

Corresponding Author:
Source of support:

* Chenyang Ma and Juying Zhou contributed equally to this work and thus shared the co-first authorship
Yu Tu, e-mail: tuyu_88@sina.com
This study was supported by the National Natural Science Foundation of China (No: 81372921 and No. 81302384)

Background: The aim of this study was to construct a radiation-induced brain injury (RBI) model and assess the effects of human recombinant endostatin in the treatment of RBI.





Material/Methods: In this study, the RBI model was used. Real-time quantitative polymerase chain reaction, immunohistochemistry, hematoxylin and eosin staining were conducted to detect the mRNA and protein expression of vascular endothelial growth factor (VEGF) and assess the effects of human recombinant endostatin in the treatment of RBI.

Results: In this study, we successfully constructed a RBI model. VEGF mRNA expression was decreased after human recombinant endostatin treatment; however, VEGF protein secretion was increased in brain endothelial cells, and the secretion of VEGF protein was decreased in glial cells and nerve cells. Body weight changes indicated that human recombinant endostatin can increase the risk of weight loss. Brain water content results showed that human recombinant endostatin might aggravate cerebral edema in the acute stage of RBI, but it can reduce the progression of cerebral edema in the early delayed stage. Survival analysis showed that human recombinant endostatin improved the survival rate only in the early stage of RBI.

Conclusions: Radiation can induce vasogenic edema and is associated with the RBI occurrence and development. VEGF protein is highly relevant to the induction of edema and thrombosis in the acute phase of RBI and in the early delayed phase of RBI, including vascular repair and regeneration, thrombus ablation and other events. Human recombinant endostatin can reduce the progression of cerebral edema during the early onset of RBI.

MeSH Keywords: **Abnormalities, Radiation-Induced • Brain Edema • Brain Injuries • Endostatins**

Full-text PDF: <https://www.medscimonit.com/abstract/index/idArt/917537>

 4162  —  8  31



Background

Radiation-induced brain injury (RBI) is a continuous and dynamic process and an unusual life-threatening complication after exposure to radiation therapy [1]. In clinics, RBI is divided into 3 types: acute phase, early-delayed phase, and late-delayed phase. In acute phase, RBI occurs within 2 weeks of the initiation of radiotherapy and sometimes occurs during radiotherapy. Most symptoms are transient, reversible, and can resolve on their own. In early-delayed phase, RBI develops 2 weeks to 6 months after irradiation. Early-delayed symptoms may be associated with disruption of the blood-brain barrier or selective oligodendrocyte dysfunction, including sleepiness syndrome, deterioration of prior symptoms, and transient cognitive impairment. In late-delayed phase RBI appears perhaps several months to years after irradiation. Late symptoms are characterized by leukoencephalopathy syndrome and mild to moderate cognitive impairment, irreversible and destructive [1–3]. Although extensive efforts have been devoted to exploring the mechanisms of RBI corresponding to clinical manifestations in the past decades, the underlying mechanism remains unclear. Currently, there have been 2 major theories which were widely recognized. The first theory is that direct damage to brain parenchymal cells is predominant, while changes in the vascular system are relatively minor. The second theory is that radiation-induced vascular damage is the most important and causes cerebral ischemia [4].

Vascular endothelial growth factor (VEGF) has been identified as the major vascular permeability regulator of microvascular permeability [5]. It has broad biological functions, such as the mediation of angiogenesis, vasculogenesis, vascular permeability, vascular remodeling, vascular survival, arterial differentiation, neurotrophic activity, hematopoiesis, and inflammatory responses [6,7]. In certain pathological conditions, such as middle cerebral artery occlusion (MCAO) [8] and brain injury [9], VEGF is significantly elevated in the marginal zone of the lesion. Increased VEGF can induce leakage of the blood-brain barrier, which can promote and aggravate the formation of cerebral edema [10–12]. A previous study also reported that treatment of rats in the early stage of cerebral ischemia with VEGF protein can increase blood-brain barrier permeability and even cerebral hemorrhage, whereas the use of VEGF inhibitors can reduce blood-brain barrier permeability [13].

Human recombinant endostatin has been expressed and purified in *Escherichia coli* [14]. It can suppress VEGF-stimulated proliferation, migration, and tube formation of human umbilical vein endothelial cells *in vitro* [14]. A previous study demonstrated that human recombinant endostatin can promote the efficacy of radiotherapy on esophageal cancer, which may be partly realized by inhibiting the activity of VEGF related signal pathways [15]; and enhancing the radio-response on esophageal

squamous cell carcinoma by normalizing tumor vasculature and reducing hypoxia [16]. However, little research has been performed on human recombinant endostatin treatment for RBI.

Research on RBI has benefited from using animal models. Particularly, rats have been used to elicit a variety of pathological changes (e.g., vascular lesions, edema, necrosis, and demyelination) [1]. In this study we used Sprague Dawley (SD) rats to construct a whole-brain irradiation model to investigate the effect of human recombinant endostatin in the treatment of RBI and evaluated its feasibility.

Material and Methods

Animals and groups

Male SD rats, weighing 250 ± 10 g, were purchased from Soochow University. They were housed in a pathogen-free environment ($22 \pm 2^\circ\text{C}$, $55 \pm 10\%$ humidity and 12/12 hours of light-dark cycle) with free access to a standard laboratory diet and water. The Medical Laboratory Animal Ethics Committee of The First Affiliated Hospital of Soochow University (no. 128) approved the animal experimental procedures.

When constructing the RBI model, animals were divided into 2 groups: 1) the sham group animals received anesthesia but not irradiation and 2) the irradiation group (IR) animals received anaesthetized and underwent whole-brain irradiation. In the experiments that investigated the efficacy of human recombinant endostatin in the treatment of RBI, animals were randomized into 4 groups: 1) the sham group animals received anesthesia but not irradiation on day 1 and were then intraperitoneally injected with saline (2 mL/kg body weight) for 14 successive days; 2) the irradiation group (IR, animals received anaesthetized and underwent whole-brain irradiation on day 1; 3) the human recombinant endostatin group (EN) animals were intraperitoneally injected with human recombinant endostatin (2 mL/kg body weight) for 14 days; and 4) the irradiation+human recombinant endostatin group (IR+EN) animals received irradiation on day 1 and were then intraperitoneally injected with recombinant human endostatin (2 mL/kg body weight; Shandong Simcere-Medgenn Bio-Pharmaceutical Co., Ltd., China) for 14 successive days. The sampling time points for the sham, IR, and IR+EN groups were 1, 3, 7, 14, 28, 42, and 56 days after irradiation, while the sampling time points for the EN group were on days 14, 28, 42, and 56 days after administration. There were 3 rats in each group at each time point.

Whole-brain irradiation

After an acclimatization period of 2 weeks, the animals received either whole-brain irradiation or sham control. Each rat



Figure 1. Whole brain irradiation model.

was anaesthetized by the intraperitoneal injection of 25% urethane solution (4 mL/kg body weight). Whole-brain irradiation was administered using a 6 MV electron beam (Siemens, Germany) to establish the animal model of RBI with a single, fractionated dose of 20 Gy. Dosimetry was performed using thermoluminescence dosimeters placed in the skulls of dead rats and confirmed using ionization chambers in tissue-equivalent phantoms. The rats received 20 Gy at an average dosage of 2 Gy/minute at a source-skin distance of 100 cm. Figure 1 shows the whole-brain irradiation procedure.

Hematoxylin and eosin (H&E) staining

Tissue sections were decarboxylated in xylene and rehydrated in a series of ethanol solutions. After rinsing with distilled water, it was stained with Harris hematoxylin solution for 5 minutes, rinsed with tap water, and stained with eosin-phloxine solution for 2 minutes.

Immunohistochemistry

At room temperature, tissue sections were blocked at 3% H₂O₂ for 10 minutes, then dewaxed, rehydrated, dehydrated, and incubated overnight at 4°C with anti-VEGF antibody (1: 20 00, ab1316, Abcam, UK). The next day, the sections were washed 3 times and incubated with a FITC-conjugated secondary antibody at 37°C for 1 hour. Sections were counterstained with hematoxylin. For quantitative data analysis, the mean integrated optical density (IOD) values of the cells were measured by Image Pro Plus 6.0 (Media Cybernetics, USA). The mean IOD value=IOD/area. The IOD and area of positive cells delineated manually were measured from a randomly selected area of 400×magnification in each visual field. The average IOD value from 10 visual fields for each section was used as the IOD value of VEGF-positive cells.

Real-time quantitative polymerase chain reaction (RT-qPCR) analysis

Total RNA was isolated from brain tissue using TRIzol reagent (Invitrogen, USA) and then reverse-transcribed to cDNA using a Prime Script™ RT Reagent Kit (TaKaRa, Japan). Subsequently, RT-qPCR was performed using an ABI Prism 7500 Sequence Detection System (7500, Applied Biosystems, USA). The thermocycling conditions were as follows: 95°C for 5 minutes; 30 cycles of 95°C for 30 seconds, 56°C for 30 seconds and extension at 72°C for 1 minute. Relative quantities of mRNA were calculated using the 2^{-ΔΔCt} method [17] and normalized to the house-keeping gene β-actin. The primer sequences were as follows: VEGF sense, 5'-GCTGTGTGTGTGAGTGGCTTA-3' and antisense, 5'-CCCATTGCTCTGTACCTTGG-3'; GAPDH sense, 5'-GCTGTGTGTGTGAGTGGCTTA-3' and antisense, 5'-CCCATTGCTCTGTACCTTGG-3'.

Brain water content (BWC)

Brain water content (BWC) was determined by the wet/dry (W/D) weight method. The skull was opened via a midline incision, and the brain was removed after euthanasia. Samples were wrapped in pre-weighed aluminum foil and immediately weighed using an electronic analytical balance to obtain the wet weight (WW), dried for 12 hours in an oven at 110°C and weighed again to obtain the dry weight (DW). BWC was estimated as follows: BWC (%)=(WW-DW)/WW×100%.

Statistical analysis

SPSS 19.0 (IBM, USA) was applied to analyze all data. Differences among multiple groups were statistically analyzed using one-way ANOVA and post hoc comparisons (Bonferroni test). Survival rates were estimated by using the Kaplan-Meier method, and *P* values were calculated using log-rank tests among the groups. Values of *P*<0.05 were considered statistically significant.

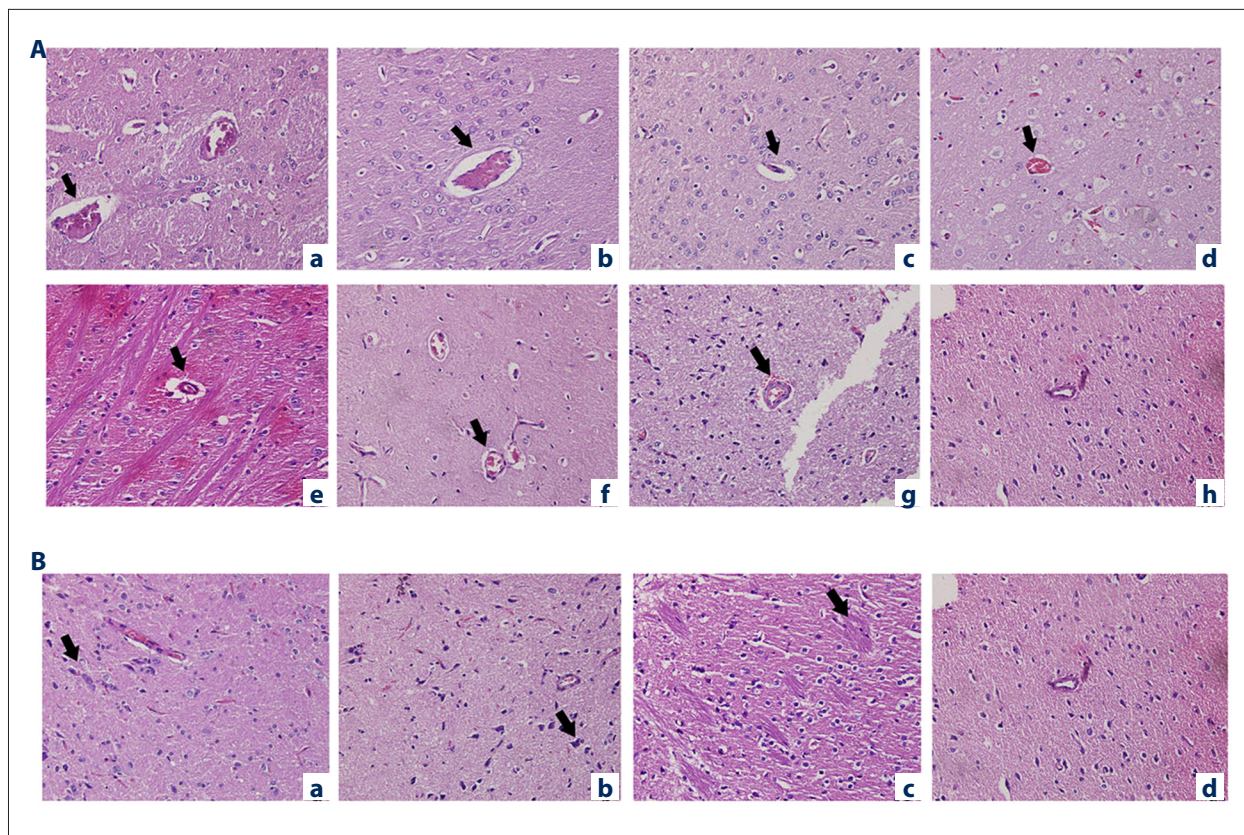


Figure 2. Hematoxylin and eosin staining results in rat cortical area after irradiation. **(A)** Pathological changes in cerebral microvascular and endothelial cells. **(a–g)** Brain tissue sections at 1, 3, 7, 14, 28, 42, and 56 days after irradiation; **(h)** brain tissue sections of Sham group. **(B)** Pathological changes in neurons, glial cells, and myelin sheath at 56 days of after irradiation.

Results

Pathological changes in cerebral microvascular and endothelial cells

On day 1 after irradiation, the cerebral capillary space was widened, and the intima was ruptured in the IR group when compared with that in the sham group. In addition, some of the blood vessels began to form thrombi, and the diameter of the unobstructed blood vessels was expanded. On day 3 to 7 after irradiation, the IR group experienced a peak of thrombosis accompanied by further widening of the vascular space and the necrosis of endovascular cells. On day 14 after irradiation, thrombus revascularization occurred in the IR group, which was accompanied by the regeneration of capillaries. On day 42 after irradiation, the blood vessel space in the IR group narrowed to the same width as that in the sham group. On day 56 after irradiation, the vascular endothelial cells showed hyperplasia, the intima of the blood vessels gradually thickened, the lumen of the blood vessels also began to narrow, and a small amount of red blood cells leaked from the damaged blood vessels. The necrotic vascular endothelial cells in the IR group were phagocytized by microglia and eventually evolved into gitter cells (Figure 2A).

Pathological changes in neurons, glial cells, and myelin sheath structure

Figure 2B shows the results of the H&E staining of neurons, glial cells, and myelin sheaths at the observation endpoint. Compared with the control group, neuronal loss occurred around the neurons, microglia neutrophils in the IR group. In the white matter, there was a small amount of water in the myelin gap, and some glial nodules formed by microglial hyperplasia were observed. In the IR group, microglia were responsible for phagocytic functions throughout the whole process, including the phagocytic degeneration of brain endothelial cells (BEC) and neurons, and eventually evolved into lattice cells.

BWC changes in the RBI model

As shown in Figure 3, there was no significant change in the BWC of the IR group from 1 to 7 days after irradiation compared with that of the sham group. At 14 days after irradiation, the BWC of the IR group reached its peak. Compared with the sham group, the BWC of the IR group increased significantly from 14 days after irradiation, and those on day 14 and day 28 were statistically significant ($P < 0.001$).

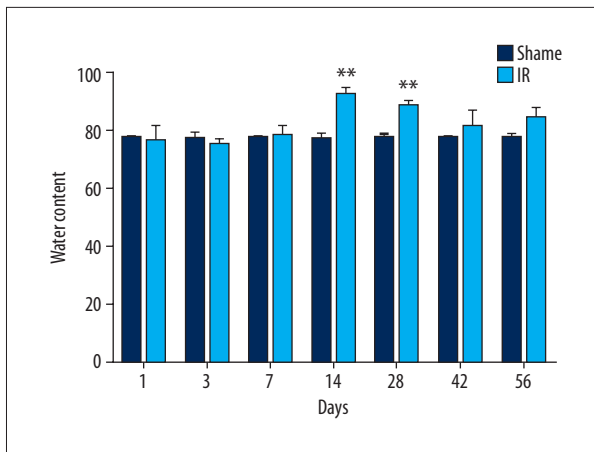


Figure 3. Determination of brain water content in a rat model with whole brain irradiation.

VEGF mRNA and protein expression in the RBI model

VEGF mRNA in the IR group showed a decreased value on day 3 after irradiation compared with that on day 1, followed by a gradual increase in expression, and reached a peak on the

day 14. However, compared with the sham group, it was significantly downregulated during the whole observation period, with statistically significant decreases on days 1, 3, 7, 28, and 42 ($P < 0.005$; Figure 4C).

Immunohistochemistry showed the localization and expression of VEGF in cells. As shown in Figure 4A and 4B, compared with the sham group, vascular endothelial cells, glial cells and nerve cells (G&N) in the IR group showed positive VEGF expression on day 1 after irradiation. In addition, VEGF expression peaked on day 14 after irradiation in different cells. This result is also consistent with the previous BWC results. In the later observation period, positive staining of VEGF in BEC and G&N persisted in the IR group (Figure 4A, 4B).

To more accurately verify the expression of VEGF in different cells, we examined changes in the IOD. Figure 4E shows changes in the VEGF IOD in G&N, and Figure 4D shows changes in the VEGF IOD in BEC. By analyzing the data, we found that the IOD of VEGF protein in G&N in the IR group was increased compared with that in the sham group, with statistically significant increases at days 1, 14, 42, and 56 ($P < 0.05$).

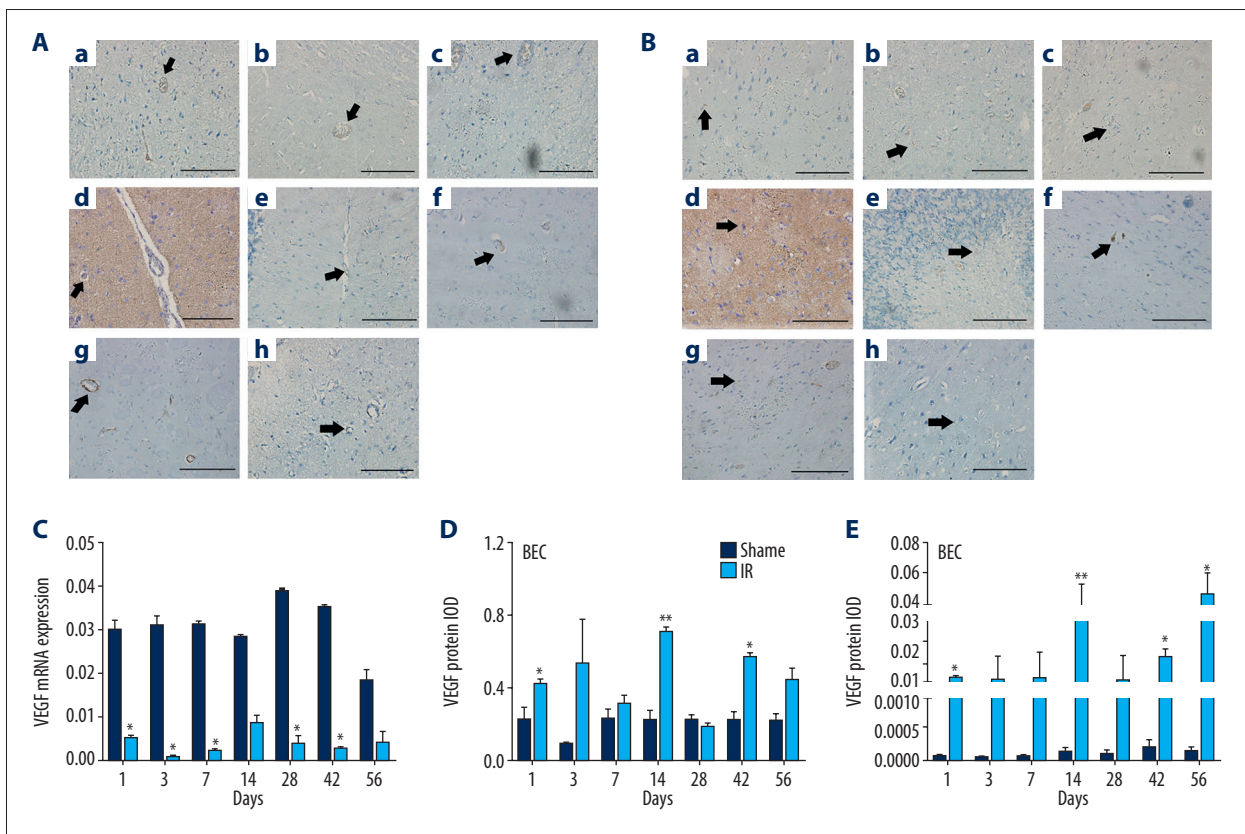


Figure 4. VEGF mRNA and protein expression in the RBI model. (A) Immunohistochemistry results of VEGF in BEC. (B) Immunohistochemistry results of VEGF in G&N. (C) VEGF mRNA expression in IR group. (D) VEGF protein IOD in BEC. (E) VEGF protein IOD in G&N. VEGF – vascular endothelial growth factor; BEC – brain endothelial cells; G&N – glial cells and nerve cells.

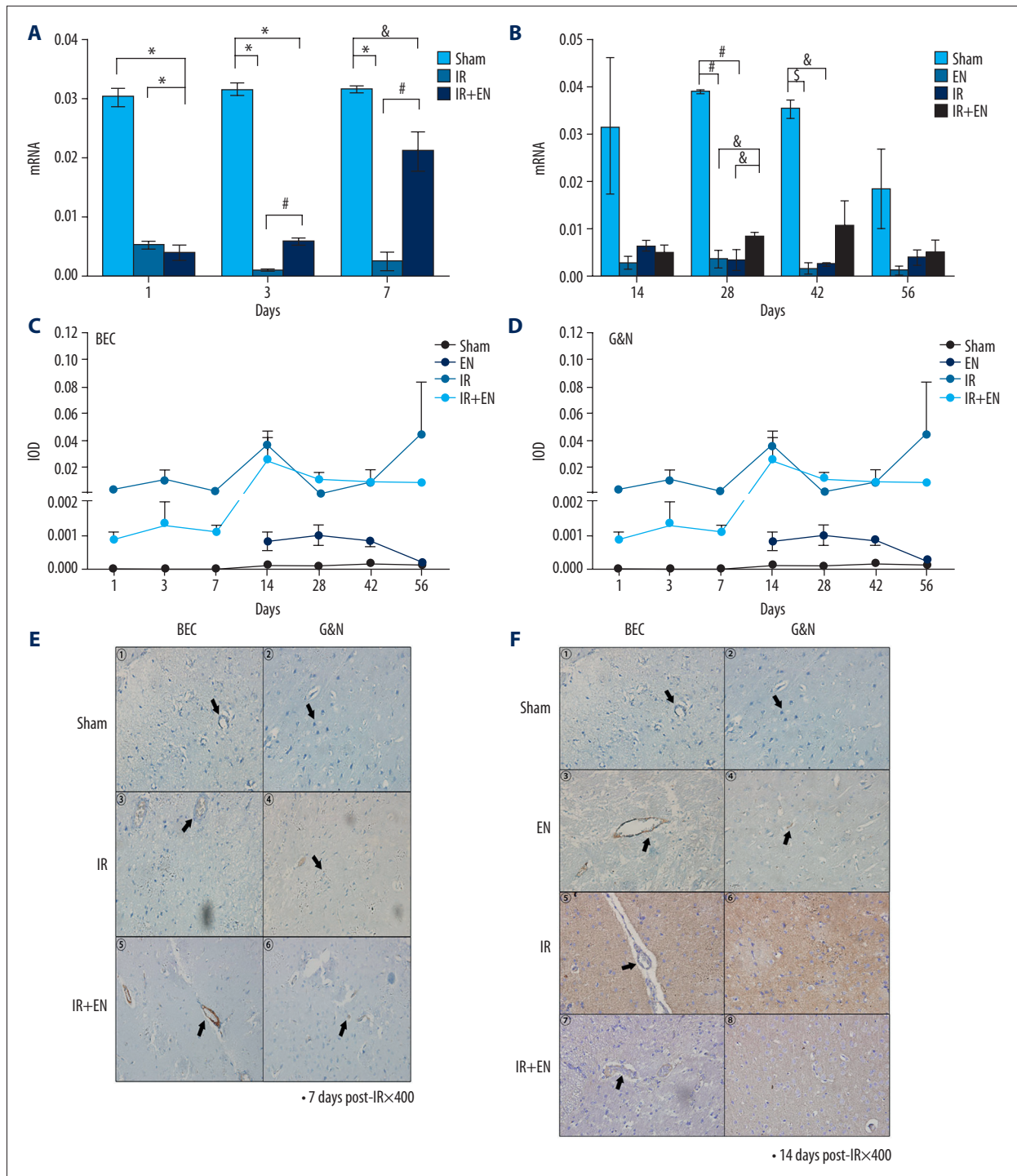


Figure 5. VEGF mRNA and protein expression changes in brain tissues post-irradiation with human recombinant endostatin treatment.

(A) VEGF mRNA expression changes in brain tissues post-irradiation with human recombinant endostatin treatment at 1, 3 and 7 days. (B) VEGF mRNA expression changes in brain tissues post-irradiation with human recombinant endostatin treatment at 14, 28, 42, and 56 days. (C) VEGF protein IOD in BEC. (D) VEGF protein IOD in G&N. (E, F) The distribution of VEGF staining positive BEC and G&N in each group on the day 7 and day 14 after irradiation. VEGF – vascular endothelial growth factor; BEC – brain endothelial cells; G&N – glial cells and nerve cells.

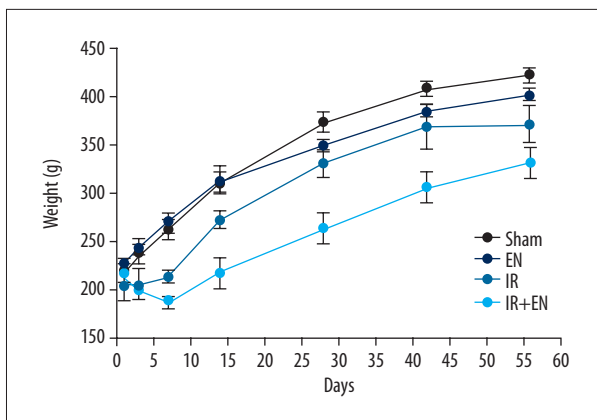


Figure 6. Changes in BWC after human recombinant endostatin treatment on the RBI model. BWC – brain water content; RBI – radiation-induced brain injury.

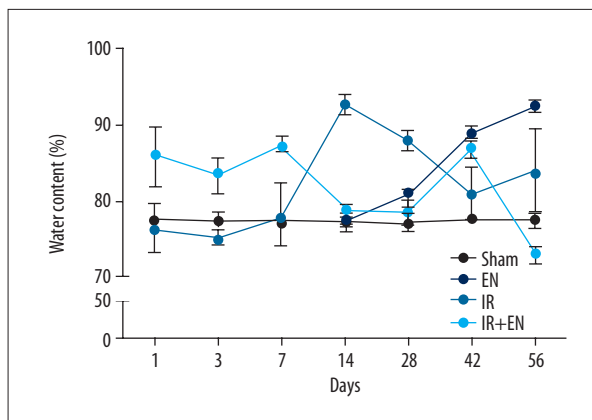


Figure 7. Changes in weight after human recombinant endostatin treatment on the RBI model. RBI – radiation-induced brain injury.

However, in BEC, the VEGF IOD was increased except on day 28 compared with that in the sham group, with statistically significant increases on days 1, 14, and 42 ($P < 0.05$). Both IOD elevations were time dependent.

VEGF mRNA and protein expression changed in brain tissues post-irradiation with human recombinant endostatin treatment

As shown in the line graph (Figure 5A), VEGF mRNA expression in the IR+EN group was lower than that in the sham group during the whole observation period. The differences were statistically significant at 1, 3, and 7 days after irradiation ($P < 0.005$). Compared with the IR group, VEGF mRNA expression in the IR+EN group was increased significantly at day 3 ($P = 0.0030$), day 7 ($P = 0.0010$), and day 28 ($P = 0.047$). Compared with the EN group, the mRNA expression of VEGF in the IR+EN group was higher at each time point, but there was a significant difference between them only on day 28 ($P = 0.0240$).

To further detect the expression of VEGF after human recombinant endostatin treatment, we carried out a quantitative analysis of the protein expression of VEGF in BEC and G&N. In the IR+EN group, the IOD of VEGF in BEC was higher than that in the sham group at each time point. Compared with the IR group, it was statistically significant on days 7, 42, and 56 after irradiation ($P < 0.005$) (Figure 5B). However, the mean IOD of VEGF in G&N was statistically significant only on day 28 after irradiation compared with that in the IR group (Figure 5C) ($P < 0.005$).

In addition, we can also see from the line graph that the average IOD of VEGF protein in BEC reached its peak on day 7 after irradiation and that of VEGF protein in G&N reached its peak on day 14 after irradiation. Correspondingly, we compared and analyzed the H&E staining results of BEC and G&N on days 7 and 14, respectively. H&E staining showed that

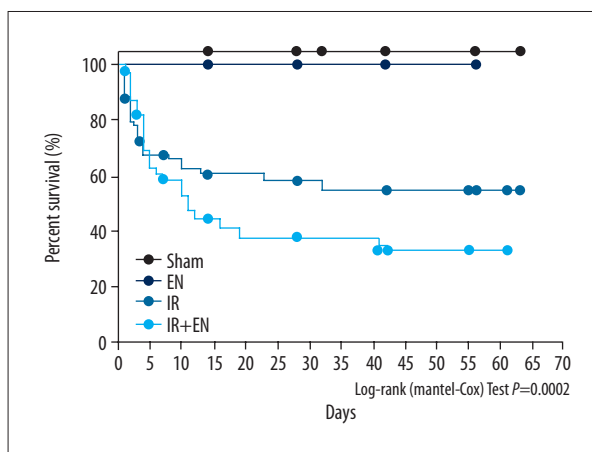


Figure 8. Survival rate analysis after human recombinant endostatin treatment on the RBI. RBI – radiation-induced brain injury.

human recombinant endostatin used in RBI treatment can induce BEC to upregulate the secretion of VEGF protein; on the contrary, it can reduce the secretion of VEGF protein in G&N (Figure 5D, 5E).

Body weight changed after irradiation with human recombinant endostatin treatment

No significant differences in body weight growth were observed between the sham and EN groups throughout the observation period. Compared with the weight growth of the rats in the aforementioned 2 groups, the body weight in the IR group and the IR+EN group decreased significantly from day 3 after irradiation until the end of the observation period. Compared with the IR group, the body weight of the rats in the IR+EN group were significantly decreased from day 7 after irradiation to the end point of observation, with statistical significance ($P < 0.005$) (Figure 6).

Brain water content changed after irradiation with human recombinant endostatin treatment

As shown in Figure 7, BWC in the IR+EN group increased significantly on day 3, 7, and 44 after irradiation, with statistical significance ($P<0.005$) compared with the sham group and the IR group. However, it was significantly lower than that in the IR group on day 14 and day 28 after irradiation ($P<0.05$) and significantly lower than that in the EN group and the IR group at the observation endpoint ($P<0.05$).

Survival rate analysis

The survival rates of the rats in the sham group and the EN group were 100% during the observation period, and both groups had higher survival rates than those of the IR group and the IR+EN group. On day 4 day after irradiation, the survival rate of the IR+EN group was 68.83%, which was significantly higher than that of the IR group (67.47%; log-rank tests: $P=0.0002$). However, the survival rate of the IR+EN group was lower than that of the IR group on day 5 after irradiation. At the end of observation period (56 days after irradiation), the survival rate of the IR group was 54.88%, and the survival rate of the IR+EN group was only 32.76% (Figure 8).

Discussion

Radiation therapy is widely used for the treatment of various primary and metastatic malignant tumors of the brain and neck. With the development of modern clinical radiotherapeutic techniques, radiation can be delivered more precisely to the targeted tumors, limiting radiation damage to a core of diseased tissues. However, the irradiation fields associated with such therapy inevitably involve some normal brain tissues [18]. RBI can damage neurons, glial cells, and blood vessels in the brain and can cause changes in molecules, cells, and functions. [2]. To explore the potential mechanism of RBI and to identify feasible treatment methods, researchers have established animal models to explore the histopathology of the pathogenesis of brain injury. In the study of radiological brain injury, animal models were used to reveal a variety of pathological changes (e.g., angiopathy, edema, necrosis, and demyelination) [1]. In this study, we used rats to construct a brain injury model and observed the pathological changes in cells after radiation and the expression changes in corresponding genes to determine whether the brain injury model was successfully constructed.

RBI includes glial atrophy, demyelination, necrosis, varying degrees of vascular changes, and other histopathological alterations. Yuan et al. showed that radiation would cause an enlargement of the nucleus of the brain endothelium, the dilatation

of blood vessels, the contraction of blood vessel walls, a decrease in blood vessel density and length, and an increase in blood vessel permeability [19]. Raber et al. showed that whole-brain single or fractionated irradiation of young adult mice and rats led to a significant decrease in newborn, mature and immature neurons in the dentate gyrus (DG) [20] and Li et al. showed that radiation can lead to demyelination and white matter necrosis and promote glial cell apoptosis [21]. In our study, we obtained similar results by H&E staining.

The tissue D/W ratio method is one of the most commonly used indicators to measure tissue water content [22]. This part of the experiment used the D/W ratio of brain tissue to study the change trend of brain edema in the RBI model group. Baldwin et al. [23,24] believed that the blood-brain barrier would be opened for the first time within 24 hours after brain injury and for the second time after brain injury on day 3. In this experiment, BWC in the IR group did not increase significantly 1 to 7 days after irradiation compared with the sham group. Combined with the results of H&E staining, cerebral capillary thrombi gradually formed on day 1 after irradiation and peaked on day 3. Therefore, we believe that the nonsignificant increase in the BWC in the first 1 to 7 days after RBI is mainly related to the relative closure of the blood-brain barrier, which may be caused by cerebral microcirculation disorder and cerebral blood flow hypoperfusion. However, starting at 14 days after radiation, the BWC in the IR group was significantly higher than that in the sham group and reached a peak at day 14. This result indicated that the peak of brain edema in the RBI model occurred at the second week after exposure, and it also showed that the period of brain edema in the RBI model coincided with the clinical occurrence of the acute phase of brain edema in the RBI model (that is, it often occurred within days to weeks after exposure) [1]. Moreover, H&E staining showed that intracranial capillary thrombosis appeared to undergo mechanized recanalization on day 14 after irradiation. This observation indicates that the relative increase in the BWC in the IR group is closely related to thrombus recanalization and a biphasic change in the blood-brain barrier, but the specific mechanism needs to be explored in the next step.

VEGF also known as vascular permeability factor (VPF), is an important angiogenic cytokine. It regulates proliferation, differentiation, and survival of endothelial cells and enhances vascular permeability [25]. It was shown that the overexpression of vascular VEGF is an outstanding manifestation in the course of RBI [26]. Lee et al. [27] found that VEGF mRNA showed a significant decrease 8 hours after irradiation, which was accompanied by an increased apoptosis rate and a decreased proliferation rate of brain endothelial cells. They believed that the downregulation of the VEGF gene induced by radiation promoted endothelial cell apoptosis and slowed the proliferation of endothelial cells through the ang-2 pathway,

which eventually led to a significant decrease in the number of cerebral microvessels. By detecting the mRNA expression level of VEGF, we found that the mRNA expression of VEGF was decreased in the IR group from the first day after irradiation and continued throughout the observation period, which indicated that the transcriptional function of the VEGF gene in the RBI model was relatively inhibited. In combination with the first part of the pathological results, we believe that the inhibition of VEGF gene expression is closely related to endothelial cell injury and apoptosis. In normal mature brain tissue, there is little expression of VEGF protein, which is generally only found in areas with abundant blood vessels in the brain, such as the choroid plexus, ependyma, pituitary gland, and cerebellar granulosum cells. Under the conditions of hypoxia, ischemia, trauma, tumor, demyelination, and other conditions, the expression of VEGF protein in brain tissue is significantly increased [28,29]. In our study, immunohistochemical results showed that BEC VEGF protein in the IR group was upregulated from the first day after irradiation, and pathological results also showed endothelial cell injury and thrombosis. On day 14 after irradiation, the expression of VEGF protein in BEC and G&N in the IR group continued to rise to the peak, which coincided with the timing of cerebral edema at the peak, and the intracerebral capillary thrombus began to be recanalized with angiogenesis. Meanwhile, immunohistochemical quantitative analysis also proved that high VEGF expression can promote the occurrence of angiogenesis and cerebral edema. Due to the non-strict linear relationship between mRNA and protein expression, the expression of VEGF mRNA and protein might be out of sync after RBI. Based on the aforementioned results, we speculate that VEGF is involved in the induction of edema and thrombosis in the acute phase of RBI, and in the early delayed phase of RBI, it is involved in vascular repair and regeneration, thrombus ablation, and other events.

Human recombinant endostatin is an analogue of endostatin, a naturally occurring endogenous inhibitor of neovascularization, that has been widely used in anti-angiogenesis therapy for cancer. Studies have shown that human recombinant endostatin can inhibit TNF- α -induced receptor activator of NF- κ B ligand expression in fibroblast-like synoviocyte [30], and directly inhibit the expression of VEGF protein [31]. Anti-VEGF therapy has some therapeutic benefit in RBI therapy, although certain therapeutic side effects and specific mechanisms are unknown. Therefore, on the basis of the animal model of RBI, we added human recombinant endostatin treatment to explore the feasibility of anti-VEGF measures in the treatment of RBI. In our study, compared with the sham group, VEGF mRNA in the IR+EN group was downregulated throughout the observation period. However, compared with the IR group, VEGF mRNA increased significantly on days 1, 3, 7, and 28. This result did not support the hypothesis that endostatin reduces vascular

permeability. Furthermore, the BWC results showed that endostatin induced more severe cerebral edema. This conclusion suggests that human recombinant endostatin, applied in RBI model rats, has a limited role in the control of acute cerebral edema in the early stage of RBI, which also indicates that there might be other signal transduction pathways to initiate cerebral edema and the upregulation of VEGF mRNA and protein expression. Therefore, further study is needed. In the IR+EN group, the expression of VEGF protein in BEC showed a slight rebound during the whole observation period, but in G&N, the expression of VEGF was relatively inhibited. The average IOD of the former was several orders of magnitude higher than that of the latter. Therefore, we believe that VEGF protein from BEC contributes significantly to total VEGF protein in the whole brain tissue and is involved in maintaining cerebral edema.

The survival curve after recombinant human endostatin intervention showed that there was no significant difference in the survival rate of rats after human recombinant endostatin treatment. The survival rate of the irradiated rats was significantly lower than that of the unirradiated rats, and the median survival time of the irradiated rats was 32 days. Meanwhile, the upper limit of BWC in the sham group, namely, <80%, was defined as the upper limit of non-brain edema. We observed that the survival rate of rats defined as having brain edema (BWC 80%) was significantly lower than that of the non-edema group, and the median survival time was 12 days. These results indicated that human recombinant endostatin improved the survival rate of experimental animals only in the early stage of RBI, but the survival rate decreased significantly from day 5 after the observation to the end point. We speculate that the influencing factors are radiation-induced brain edema. In addition, based on the change in body weight analysis, human recombinant endostatin will also increase the weight loss of mice.

Conclusions

Radiation can cause blood-brain barrier damage and induce the formation of vasogenic edema, which is involved in the development of RBI. The formation and ablation of intracerebral capillary thrombosis in the RBI model might result in cerebral blood perfusion and a bipolar change in the blood-brain barrier. Human recombinant endostatin can partially relieve cerebral edema, but the duration and long-term observation of human recombinant endostatin for RBI anti-VEGF therapy needs to be further explored in future experiments.

Conflict of interest

None.

References:

1. Yang L, Yang J, Li G et al: Pathophysiological responses in rat and mouse models of radiation-induced brain injury. *Mol Neurobiol*, 2017; 54: 1022–32
2. Balentova S, Adamkov M: Molecular, cellular and functional effects of radiation-induced brain injury: A review. *Int J Mol Sci*, 2015; 16: 27796–815
3. Jin X, Liang B, Chen Z et al: The dynamic changes of capillary permeability and upregulation of VEGF in rats following radiation-induced brain injury. *Microcirculation*, 2014; 21: 171–77
4. Hopewell JW: Late radiation damage to the central nervous system: A radiobiological interpretation. *Neuropathol Appl Neurobiol*, 1979; 5: 329–43
5. Wang Z, Wang N, Han S et al: Dietary compound isoliquiritigenin inhibits breast cancer neoangiogenesis via VEGF/VEGFR-2 signaling pathway. *PLoS One*, 2013; 8: e68566
6. Cao Y: Positive and negative modulation of angiogenesis by VEGFR1 ligands. *Sci Signal*, 2009; 2: re1
7. Dvorak HF: Vascular permeability factor/vascular endothelial growth factor: A critical cytokine in tumor angiogenesis and a potential target for diagnosis and therapy. *J Clin Oncol*, 2002; 20: 4368–80
8. Chen L, Zhu YM, Li YN et al: The 15-LO-1/15-HETE system promotes angiogenesis by upregulating VEGF in ischemic brains. *Neurol Res*, 2017; 39: 795–802
9. Tooke K, Girard BM, Vizzard MA: Functional effects of blocking VEGF/VEGFR2 signaling in the rat urinary bladder in acute and chronic CYP-induced cystitis. *Am J Physiol Renal Physiol*, 2019; 317(7): F43–51
10. Liu L, Fujimoto M, Kawakita F et al: Vascular endothelial growth factor in brain edema formation after subarachnoid hemorrhage. *Acta Neurochir Suppl*, 2016; 121: 173–77
11. Liu L, Fujimoto M, Kawakita F et al: Anti-vascular endothelial growth factor treatment suppresses early brain injury after subarachnoid hemorrhage in mice. *Mol Neurobiol*, 2016; 53: 4529–38
12. Jiang S, Xia R, Jiang Y et al: Vascular endothelial growth factors enhance the permeability of the mouse blood-brain barrier. *PLoS One*, 2014; 9: e86407
13. Zhang ZG, Zhang L, Jiang Q et al: VEGF enhances angiogenesis and promotes blood-brain barrier leakage in the ischemic brain. *J Clin Invest*, 2000; 106: 829–38
14. Ling Y, Yang Y, Lu N et al: Endostar, a novel recombinant human endostatin, exerts antiangiogenic effect via blocking VEGF-induced tyrosine phosphorylation of KDR/Flk-1 of endothelial cells. *Biochem Biophys Res Commun*, 2007; 361: 79–84
15. Liu GF, Chang H, Li BT et al: Effect of recombinant human endostatin on radiotherapy for esophagus cancer. *Asian Pac J Trop Med*, 2016; 9: 86–90
16. Zhu H, Yang X, Ding Y et al: Recombinant human endostatin enhances the radioresponse in esophageal squamous cell carcinoma by normalizing tumor vasculature and reducing hypoxia. *Sci Rep*, 2015; 5: 14503
17. Livak KJ, Schmittgen TD: Analysis of relative gene expression data using real-time quantitative PCR and the 2(-Delta Delta C(T)) method. *Methods*, 2001; 25: 402–8
18. Zhu Y, Ling Y, Zhong J et al: Magnetic resonance imaging of radiation-induced brain injury using targeted microparticles of iron oxide. *Acta Radiol*, 2012; 53: 812–19
19. Brown WR, Blair RM, Moody DM et al: Capillary loss precedes the cognitive impairment induced by fractionated whole-brain irradiation: A potential rat model of vascular dementia. *J Neurol Sci*, 2007; 257: 67–71
20. Raber J, Rola R, LeFevour A et al: Radiation-induced cognitive impairments are associated with changes in indicators of hippocampal neurogenesis. *Radiat Res*, 2004; 162: 39–47
21. Li YQ, Guo YP, Jay V et al: Time course of radiation-induced apoptosis in the adult rat spinal cord. *Radiation Oncol*, 1996; 39: 35–42
22. Benlier E, Eskioçak S, Puyan FO et al: Fucoidin, a neutrophil rolling inhibitor, reduces damage in a rat electrical burn injury model. *Burns*, 2011; 37: 1216–21
23. Baldwin SA, Fugaccia I, Brown DR et al: Blood-brain barrier breach following cortical contusion in the rat. *J Neurosurg*, 1996; 85: 476–81
24. Ferrara N: Vascular endothelial growth factor: Molecular and biological aspects. *Curr Top Microbiol Immunol*, 1999; 237: 1–30
25. Bagheri A, Kumar P, Kamath A, Rao P: Association of angiogenic cytokines (VEGF-A and VEGF-C) and clinical characteristic in women with unexplained recurrent miscarriage. *Bratisl Lek Listy*, 2017; 118: 258–64
26. Zhou D, Huang X, Xie Y et al: Astrocytes-derived VEGF exacerbates the microvascular damage of late delayed RBI. *Neuroscience*, 2019; 408: 14–21
27. Vikman P, Ansar S, Henriksson M et al: Cerebral ischemia induces transcription of inflammatory and extracellular-matrix-related genes in rat cerebral arteries. *Exp Brain Res*, 2007; 183: 499–510
28. Croll SD, Wiegand SJ: Vascular growth factors in cerebral ischemia. *Mol Neurobiol*, 2001; 23: 121–35
29. Pilitsis JG, Rengachary SS: Complications of head injury. *Neurol Res*, 2001; 23: 227–36
30. Gao QF, Zhang XH, Yuan FL et al: Recombinant human endostatin inhibits TNF-alpha-induced receptor activator of NF-kappaB ligand expression in fibroblast-like synoviocytes in mice with adjuvant arthritis. *Cell Biol Int*, 2016; 40: 1340–48
31. Zhang L, Ge W, Hu K et al: Endostar down-regulates HIF-1 and VEGF expression and enhances the radioresponse to human lung adenocarcinoma cancer cells. *Mol Biol Rep*, 2012; 39: 89–95